Isı Bilimi ve Tekniği Dergisi, 40, 1, 99-112, 2020
J. of Thermal Science and Technology
©2020 TIBTD Printed in Turkey
ISSN 1300-3615

FLOW AND FORCED HEAT TRANSFER FROM TANDEM SQUARE CYLINDERS NEAR A WALL

Özge YETİK* and Necati MAHİR**
*,**Eskişehir Osmangazi Üniversitesi, Mühendislik Mimarlık Fakültesi Makine Mühendisliği Bölümü
26480 Batımeşelik, Eskişehir
*oyetik@ogu.edu.tr, **nmahir@ogu.edu.tr

(Geliş Tarihi: 04.07.2019, Kabul Tarihi: 21.02.2020)

Abstract: In this study, the flow and heat transfer characteristics of two heated square cylinders in a tandem arrangement near a wall is investigated. The numerical computations are carried out by solving the unsteady two dimensional Navier-Stokes and energy equations. A fractional step method with Crank-Nicholson schema was employed to the convective and the viscous terms of the equations. At the inlet, fully developed laminar boundary layer is employed for longitudinal velocity over the plane wall while transverse velocity set to zero. The simulations are performed for Prandtl number (Pr) of 0.71 and Reynolds number (Re) of 150 where the flow is considered two dimensional. The flow field characteristics and heat transfer depend not only on the ratio of the space between the cylinders (L/D) but also on the distance between the cylinder center and the wall (G/D). The vorticity and isotherm curves are generated and discussed for various L/D and G/D ratios to clarify the connection with flow and heat transfer characteristics. When the cylinders are within the boundary layer formed on the plane wall, the large difference between the velocities at the upper and lower side of the cylinders leads to noticeable variation at the flow and heat transfer characteristics.
Keywords: Heat Transfer, Numerical Simulation, Tandem square cylinders, Wall effect.

DUVAR YAKININDA ART ARADA YERLEŞTİRİLMİŞ KARE KESİTLİ SİLİNDİRLER ETRAFINDA AKIŞ VE ZORLANMIŞ TAŞINIM İLE ISI GEÇİŞİ

Özet: Bu çalışmada bir duvar yakınında arka arkaya yerleştirilmiş ısıtılmış kare kesitli silindirler etrafındaki akışın karakteristiklerini ve ısı geçişi incelenmiştir. Hesaplamalar zamana bağlı 2-boyutlu Navier Stokes ve enerji denklemlerinin çözümü ile gerçekleştirilmiştir. Denklemlerin viskoz ve taşınım terimleri için Cranck-Nicholson şeması ile birlikte kısmi adımlar metodu kullanılmıştır. Girişte duvara paralel hız bileşeni için tam gelişmiş laminar sınır tabaka kullanılmış, akışa dik yönünde hız bileşeni sıfır olarak alınmıştır. Simulasyonlar 0.71 Prandtl (Pr) sayısı ve akışın iki boyutlu olduğu Reynolds (Re) sayısının 150 değeri için gerçekleştirilmiştir. Akış karakteristikleri ve ısı geçişi yalnızca silindirler arasındaki uzaklık (L/D) ye değil aynı zamanda silindirlerin merkezi ile duvar arasındaki uzaklığa da (G/D) bağlıdır. Akış ve ısı geçişi arasındaki bağlantıyı ortaya çıkarmak için değişik L/D ve G/D oranları için çevrinti ve eş sıcaklık eğrileri elde edilmiş ve tartışılmıştır. Silindirler duvardan oluşan sınır tabakanın içerisinde kaldığında, silindirlerin üst ve alt yüzeyindeki hızlar arasındaki büyük fark akış ve ısı geçiş parametrelerinde önemli değişimlere neden olmuştur.
Anahtar Kelimeler: Isı geçiş, sayısal simulasyon, art arda kare kesitli silindirler, duvar etkisi.

NOMENCLATURE

C_D	drag coefficient
C_L	lift coefficient
D	cylinder length [m]
f	vortex shedding frequency [Hz]
F_D	drag force [N]
F_L	lift force [N]
G	gap between cylinder center and the plane wall [m]
Grad	gradient
H	advection
h	local heat transfer coefficient [W/m^{2}K]
k	conductivity [W/mK]
L	distance between cylinders [m]
Lap	laplacian
n	time step
Nu	Nusselt number [= hD/k]
P	dimensionless pressure [= $P^*/\rho U^2$]
Pr	Prandtl number [= ν/α]
r	normal direction
Re	Reynolds number [= UD/ν]
St	Strouhal number [= fD/U]
T	dimensionless temperature $\left[(T^* - T^*_\infty)/(T^*_w - T^*_\infty)\right]$
t	dimensionless time [= t^*U/D]
U	average velocity (m/s)

u dimensionless axial velocity component [= u^*/U]
u_c average velocity [m/s]
V dimensionless velocity [= V/U]
v dimensionless normal velocity component [v^*/U]
x dimensionsless axial coordinate [= x^*/D]
y dimensionsless normal coordinate [= y^*/D]

Greek symbols

α thermal diffusivity [m^2/s]
δ boundary layer thickness [m]
Φ pressure correction
ϕ intermediate velocity and pressure correction
ν kinematic viscosity [m^2/s]
ρ density [Kg/m^3]
τ shear stress [Pa]

Subscripts

b back surface
f front surface
rms root mean square
tp top surface
w wall
1 upstream cylinder
2 downstream cylinder
∞ free stream

INTRODUCTION

Unsteady flow around the bluff bodies are extensively studied in the past because of their many practical applications. Heat exchangers, offshore pipelines in close proximity to the seabed, electronic cooling are some of the application areas encountered as tandem or side by side in arrangement. The succession of the two cylinders complicates the flow in the downstream region. Existence of the wall near these cylinders also leads the flow to become more complex. The heat transfer from the cylinders is also affected by the complex structure between the cylinders and in the downstream region. Much of the studies related to the flow around the bluff bodies are about a single cylinder located in a free stream. Robichaux et al. (1999), Franke et al. (1990), Shimizu and Tanida (1978), Sohankar et al. (1998) are studied 2-D and 3-D flow structures and the variation of flow parameters for the Reynolds number ranging from 100 to 250. Sharma and Eswaran (2004) studied flow structure from a square cylinder and the study also includes forced heat transfer for both uniform heat flux and constant cylinder temperature. The effects of the Reynolds and Prandtl number on the heat transfer from a square cylinder also investigated by Sahu et al. (2009) for constant cylinder temperature and heat flux.

The flow characteristics behind the cylinder placed near a plane wall have been studied by many researchers (Bhattacharyya and Maiti (2004), Malavasi and Trabucchi (2008), Samani and Bergstrom (2015), Wang and Tan (2008), Mahir (2009)). Studies focus mainly on interactions of shear layers formed from both cylinder and wall when the cylinders placed near the wall. Wang and Tan (2008) investigated flow characteristics behind a circular cylinder placed close to wall at the difference boundary layer thicknesses (δ) for Reynolds number (Re) of 1.2×10^4. They observed Karman-like vortex shedding for the distances between the cylinder and wall (G/D) is larger than 0.3, however the wake is asymmetric about the cylinder centerline for G/D ≤ 0.6. Mahir (2009) focused on the 3-D flow and investigated the vortex structure and unsteady forces on the square cylinder placed close to the plane wall. In this study the Reynolds number range was 155-250 where between the transition from 2-D to 3-D flow takes place. Wang et al. (2014) studied flow around a square cylinder near a plane wall for Re = 6300. They categorized flow structure relating to cylinder-wall spacing.

For tandem arrangements, the flow structures are more complicated than the single one due to the unsteady flow between the cylinders and in the gap region of cylinders-wall. The studies on the tandem cylinders mostly focus on the identification of flow structures. Chatterjee and Mondal (2012) performed numerical simulations to investigate forced convective heat transfer from isothermal tandem cylinders in the free stream of air. In their study Reynolds number ranges from 50 to 150 while the gap between the cylinder varies from 1D to 10D. They observed a discontinuous jump at the drag coefficient on the downstream cylinder at the critical cylinder spacing where vortex formed between cylinder. Time average drag coefficients and Nusselt numbers have higher values on the upstream cylinder than that on downstream. Sohankar and Etminan (2009) performed numerical simulation on the flow characteristics and heat transfer over isothermal tandem square cylinders. They ranged the Reynolds number from 1 to 200 while keeping the cylinder spacing and the Prandtl number (Pr) constant as 5D and 0.71, respectively. They found that the heat transfer is higher from the front surface while is the lowest on the back surface. At the given cylinder spacing, heat transfer from upstream cylinder was relatively similar to that from the single cylinder. Mahir and Altaç (2008) performed numerical simulation to study convective heat transfer from isothermal tandem cylinders. They changed the distance between the cylinders in the range of 2D-10D while keeping the Reynolds number as 100 and 200. They provide variation of local nusselt number on the cylinders during one period of vortex formation in the downstream region. Chatterjee and Amiroudine (2010) studied numerically mixed convection heat transfer from isothermal tandem cylinders. In the study, the cylinders were confined with the blockage ratio of 10% and the Reynolds number was in the range of $1\leq Re \leq30$. They also changed Prandtl and Richardson number (Ri) in the range of $0.7\leq Pr \leq100$ and $0\leq Ri \leq1$ respectively.

There are very few investigations on the tandem cylinders near the wall. The numerical studies were performed with uniform flow or a uniform shear assumption at the inlet of computational domain. Tang et al. (2015) investigated flow structure behind the tandem

circular cylinders near the wall. In the study, they changed the gap between the wall and cylinders in the range of 0.25D-2.0D, and the distance between the cylinders as 1.0D- 4.0D while keeping the Reynolds number fixed at 200. They classified the vortex structures as no shedding mode, one-wake mode and two-wake mode. Harichandan and Roy (2012) performed a numerical study to investigate the behavior of the vertical wake behind a single and tandem cylinders placed in the boundary layer of a wall for Reynolds number of 100 and 200. They changed the gap between the wall and cylinders in the range of 0.2D-2.0D by maintaining the gap between the cylinders as 2D and 5D. They compared their result with a single cylinder near the wall and observed that flow structure in the downstream region of the tandem cylinders in the vicinity of a plane wall shows a stronger dependence on Reynolds number than gap ratio compared to that of a single cylinder. Raiola et al. (2016) experimentally investigated the near wake of two circular tandem cylinders near the wall for Reynolds number of 4.9×10^3. They chose the distance between the cylinders as 1.5D, 3D and 6D, and the cylinder-wall gap as 0.3D, 1D and 3D. For 1D wall-to-cylinder distance, the ground has strong effect on the flow field with introducing Von Kármán type wake. For the gap 0.3D, a flapping jet-type like structure forms from the gap between the cylinders and wall.

Foregoing studies deal with mainly the heat transfer from tandem cylinders in a uniform flow field and/or the flow around a single cylinder near a plane wall. The boundary layer formed on the wall close to the tandem cylinders also contributes the complexity of flow around the cylinders and convective heat transfer from them. To the best of our knowledge, we have not come across publications on the heat transfer from the cylinders in a tandem arrangement near a wall. Thus, the influence of wall proximity on heat transfer from the tandem cylinders in conjunction with the flow needs to be investigated. For this purpose; in this study the flow and convective heat transfer from tandem cylinders within and outside of an oncoming boundary layer are studied for air flow. The flow and heat transfer characteristic are computed and analyzed for the cylinder spacing (L/D) 1.5, 2.5, and 4, and cylinder center to wall distances (G/D) 0.7, 1, 1.5, 2, 2.5, 3, 3.5, 4 and 6.

GOVERNING EQUATIONS AND NUMERICAL METHOD

The transition from 2-D to 3-D takes place at the Reynolds number of about 165 (Mahir, 2009) for flow around a single cylinder. Therefore, in this study Reynolds number kept constant at 150 where the flow is 2-D. The unsteady dimensionless form of the 2-D Navier-Stokes and the energy equations are given as:

$$\frac{\partial u}{\partial x}+\frac{\partial v}{\partial y}=0 \tag{1}$$

$$\frac{\partial u}{\partial t}+u\frac{\partial u}{\partial x}+v\frac{\partial u}{\partial y}=-\frac{\partial p}{\partial x}+\frac{1}{\mathrm{Re}}\left(\frac{\partial^2 u}{\partial x^2}+\frac{\partial^2 u}{\partial y^2}\right) \tag{2}$$

$$\frac{\partial v}{\partial t}+u\frac{\partial v}{\partial x}+v\frac{\partial v}{\partial y}=-\frac{\partial p}{\partial y}+\frac{1}{\mathrm{Re}}\left(\frac{\partial^2 v}{\partial x^2}+\frac{\partial^2 v}{\partial y^2}\right) \tag{3}$$

$$\frac{\partial T}{\partial t}+u\frac{\partial T}{\partial x}+v\frac{\partial T}{\partial y}=\frac{1}{\mathrm{Re}\,\mathrm{Pr}}\left(\frac{\partial^2 T}{\partial x^2}+\frac{\partial^2 T}{\partial y^2}\right) \tag{4}$$

where u and v are the dimensionless velocity components, T and p is the dimensionless temperature and pressure in the fluid respectively, t presents the dimensionless time. Prandtl number defined as $\mathrm{Pr}=\nu/\alpha$, where ν is kinematic viscosity and α is thermal diffusivity. Re defined with respect to cylinder length D. Nondimensional form of the variables defined as

$$u=\frac{u^*}{U},\ v=\frac{v^*}{U},\ p=\frac{p^*}{\rho U^2},\ t=\frac{t^* U}{D},\ x=\frac{x^*}{D},\ y=\frac{y^*}{D},$$
$$T=\frac{T^*-T_\infty^*}{T_w^*-T_\infty^*}$$

where U is the average velocity and ρ is the density.

The numerical method presented here was used by one of the authors (Mahir, 2009) before for simulation of a single cylinder near a wall. In this study, the method is modified for tandem cylinders in proximity of a wall. Eqs. (1)-(4) were solved applying a fractional step method (Armfield and Street, 2000) including Crank-Nicolson scheme at the discretization of the convective and viscous terms in the momentum equation.
The intermediate velocities are expressed as

$$\frac{V^{n+1/2}-V^n}{\Delta t}+\left[\frac{1}{2}H\left(V^{n+1/2}\right)+\frac{1}{2}H\left(V^n\right)\right]= -Grad\left(p^n\right)+\frac{1}{Re}\left[\frac{1}{2}Lap\left(V^{n+1/2}\right)+\frac{1}{2}Lap\left(V^n\right)\right] \tag{5}$$

where H is the advection, *Grad* is the gradient, *Lap* diffusion operator and n is the time step. The nonlinear convective terms are linearized as

$$H\left(V^{n+1/2}\right)\cong\left(V^n\nabla\right)V^{n+1/2} \tag{6}$$

The Poisson equation for the pressure correction, Φ, is expressed as

$$Lap\Phi=\frac{1}{\Delta t}\Delta V^{n+1/2} \tag{7}$$

At the next time step, the velocity and the pressure are evaluated as

$$V^{n+1}=V^{n+1/2}-\Delta t\,Grad\,\Phi \tag{8}$$

$$p^{(n+1)}=p^n+\Phi \tag{9}$$

Staggered grid has been used for solving pressure, velocity and temperature components in the equations. In both momentum and energy equations, a third order upwind scheme was applied to discretize the first order derivatives in the convective terms, whereas the central-difference formula was employed for the second-order derivatives in the viscous terms. Poisson-type equations were solved using the Jacobi method with Chebyshev acceleration procedure (Mahir, 2009).

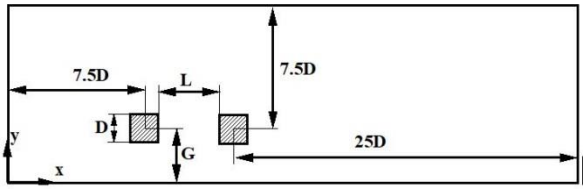

Figure 1. Computational domain and boundary locations.

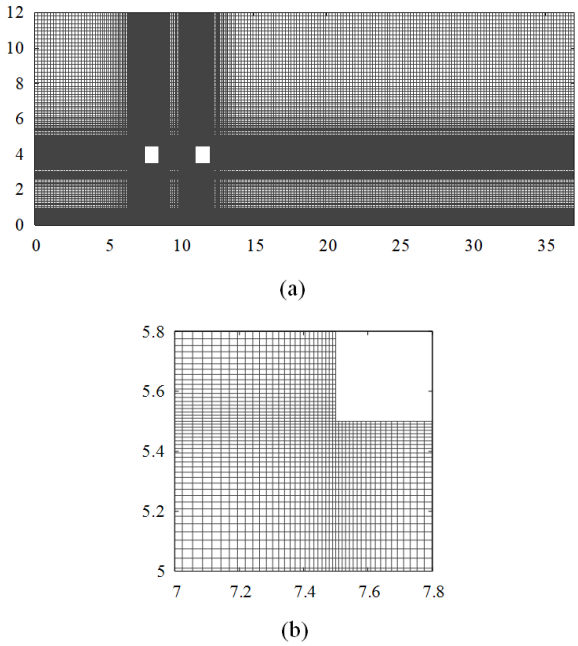

Figure 2. Grid distribution in the computation domain (a), and close-up the upstream cylinder (b).

The inflow, lateral and outflow boundaries were determined according to the Lei et al. (2000) suggestions, so that they have negligible effects on the calculated flow and heat transfer characteristics. While the upstream cylinder is placed 7.5D far from the inlet, out plane is located 25D away from the downstream one (Figure 1). The grid distribution in the computation area with the close-up view of a near corner of the upstream cylinder is presented in Figure 2. Near the cylinder walls as well as over the plane wall, dense grids are used and grid is generated in the flow field as follows. The distance of the two consecutive grid lines was determined from a geometric series. The stretching ratio (Δx_i / Δx_{i-1}, Δy_i / Δ_{yi-1}) at front and bottom of the cylinders was 0.9, while it was 1.1 at behind and over the cylinders. Grid over the plane wall is also generated with the stretching ratio of 1.1 (Mahir, 2009).

For each time step, the convergence of the iterations were determined as

$$\sum_{i,j} \frac{\left(\phi_{i,j}^{n} - \phi_{i,j}^{n-1}\right)^2}{\left(\phi_{i,j}^{n}\right)^2} < 5\times10^{-5} \qquad (10)$$

where n is time step and ϕ is the intermediate velocity and pressure correction.

At the inlet, fully developed laminar boundary layer with a third order Blasius velocity profile (Schlichting, 1979) is employed for longitudinal velocity over the plane wall. Besides, dimensionless transverse velocity and temperature also set to zero. Other boundary conditions are stated as:
No-slip condition and constant temperature on the cylinders surfaces $u = 0,\ \mathrm{v} = 0,\ T = 1$.

No-slip condition on adiabatic plane wall (at y = 0)

$$u = 0,\ \mathrm{v} = 0,\ \partial T / \partial y = 0.$$

Free slip on top boundary

$$\partial u / \partial y = \partial T / \partial y = 0,\ v = 0.$$

To minimize the distortion of the vortices at the exit, the outflow velocity is set to $\partial u / \partial t + u_c \partial u_i / \partial x_i = 0$, where u_c is average velocity. The boundary condition for the temperature is $\partial T / \partial x = 0$.

Drag and Lift force coefficients are obtained from the following expressions respectively

$$C_D = \frac{F_D}{\frac{1}{2}\rho U^2 D} \qquad (11)$$

$$C_L = \frac{F_L}{\frac{1}{2}\rho U^2 D} \qquad (12)$$

where both drag (F_D) and lift forces (F_L) are calculated by integrating the pressure and shear stresses on the cylinder surfaces.

$$F_D = \int_0^D \left(\tau_{tp}(x) + \tau_b(x)\right)dx + \int_0^D \left(P_f(y) + P_r(y)\right)dy \qquad (13)$$

$$F_L = \int_0^D \left(\tau_f(y) + \tau_r(y)\right)dy + \int_0^D \left(P_{tp}(x) + P_b(x)\right)dx \qquad (14)$$

At the equations; f, r, tp and b indicate the front, back, top and bottom surface of the cylinder. Mean values are calculated by taking average of the time history of drag, lift coefficient and Nusselt number.

The local Nusselt number (Nu) based on the cylinder length is given as

$$Nu = \frac{hD}{k} = -\frac{\partial T}{\partial r} \qquad (15)$$

where *r* is the direction normal to the cylinder surface, h is the local heat transfer coeffient and k is the thermal conductivity of fluid. The Strouhal number is expressed as follows:

$$St = \frac{fD}{U} \tag{16}$$

where *f* is the vortex shedding frequency.

The accuracy of the current program was verified by simulating a single cylinder and tandem cylinders in a free stream. First, the flow and heat transfer over the tandem cylinders were simulated. To determine the effects of different grid structures on the calculated values, the distance between the cylinders was taken as 0.5D at which no vortex formed, and 7D at which the vortex formed between them. The variation of the mean force coefficients, Nusselt and Strouhal numbers (St) with minimum grid spacing over the walls is presented in table 1 (Yetik, 2013) where the subcripts 1 and 2 correspond to upstream and downstream cylinders respectively. For both gap ratios, the smaller differences were obtained between the cases B and C. For L/D = 0.5, the mean values of C_{D1} and C_{D2} were 0.005 and 0.001 respectively while they were 0.003 for L/D = 7 Similarly, the differences at the Nu_{mean1} and Nu_{mean2} observed as 0 and 0.004, respectively, for L/D = 0.5. These values were 0.004 and 0.002, respectively, for L/D = 7. Therfore, case B is preferred at the simulations for accuracy with a convenient grid structure. Time step of $\Delta t = 0.05$ was determined to be optimum value and employed at the rest ot the simulations.

The flow and heat transfer characteristics over a square cylinder were also obtained by using the same grid structure referred for tandem cylinders and the results were compared with some the existing literature values (Tables 2-4). It is observed that the computed flow and heat transfer characteristics were in the range of the values given in the literature.

Table 1. Grid independence test for tandem cylinders in uniform flow at Re = 150.

Grid	L/D	Minimum grid interval	Grid	C_{Dmean1}	C_{Dmean2}	CL_{mean1}	CL_{mean2}	Nu_{mean1}	Nu_{mean2}	St
A	0.5	0.020	235× 153	1.382	-0.177	0.0239	-0.00040	4.139	1.831	0.152
B		0.010	340× 205	1.375	-0.169	0.0196	-0.00016	4.151	1.837	0.154
C		0.008	486× 265	1.380	-0.170	0.0174	-0.00021	4.151	1.833	0.153
A	7	0.020	309× 153	1.467	0.957	0.0245	0.0184	4.766	4.463	0.158
B		0.010	426× 205	1.463	0.931	0.0205	0.0166	4.790	4.409	0.162
C		0.008	582× 265	1.466	0.928	0.0187	0.0154	4.794	4.407	0.159

Table 2. Comparison of C_{Dmean} values for single cylinder in uniform flow.

Re	Present study	Franke et al. (1990)	Shimizu et al.(1978)	Sharma et al. (2004)	Sohankar et al. (2009)	Sohankar et al. (1998)	Sohankar et al. (1995)	Chatterjee et al. (2009)	Sahu et al. (2009)
100	1.51	1.62	1.58	1.5	1.48	1.48	1.48	1.52	1.49
120	1.48	1.59	1.54	1.45	1.45	1.45	1.42	1.47	
140	1.48	1.57	1.51	1.46	1.44	1.44	1.42	1.48	
150		1.56	1.5	1.47		1.44	1.41		
160	1.48			1.47	1.45			1.5	1.46

Table 3. Comparison of Strouhal number values for single cylinder in uniform flow.

Re	Present study	Luo et al. (2003)	Sharma et al. (2004)	Sohankar et al. (2009)	Sohankar et al. (1997)	Chatterjee et al. (2009)	Sahu et al. (2009)
100	0.151	0.147	0.149	0.146	0.143	0.145	0.148
120	0.155	0.155	0.155	0.154	0.149	0.151	
140	0.159	0.159	0.158	0.158	0.154	0.156	
160	0.162	0.157	0.159	0.161	0.156	0.159	0.16

Table 4. Comparison of mean Nu values for single cylinder in uniform flow.

Re	Present study	Sharma et al. (2004)	Sohankar et al. (2009)	Chatterjee et al. (2009)	Sahu et al. (2009)
100	4.02	4	4.2	4.05	4.3
120	4.36	4.4	4.5	4.45	4.7
140	4.66	4.75	4.75	4.75	5
160	4.93	5	5	5	5.3

RESULT AND DISCUSSION

To correlate flow structure with convective heat transfer from cylinders, the flow structure and isotherms around tandem cylinders near a wall were obtained. At the simulations, the variation of the lift and drag coefficients were provided for both cylinders. In addition to mean values, local Nusselt numbers on the cylinder surfaces also obtained.

Flow Structure and Isotherms:

In Figures 3 and 4, isovorticity curves and corresponding isotherms for various gaps (G/D) were given at the cylinder to cylinder distances of (L/D) 1.5 and 4. These cylinder to cylinder spacing were selected such that the vortex forms between the cylinders and does not form. Left and right columns present the isovorticities and the isotherms respectively for the same instances. For G/D = 0.7 and 1.0, both cylinders were inside of the boundary layer formed on the plane wall surface (Figures 3a, b). For these cases, negative vorticies are observed to be dominant in the downstream region. For G/D = 1, weak vorticies form from down surface of the both cylinders and shear layer curls at the top side of downstream region. For G/D = 1.5, the cylinders are partially inside of the boundary layer. Again, the weak positive vortex forms from down surface of the cylinders. While positive shear layer rolls between the cylinders, it loses its strength in the downstream region and negative vortex becomes dominant. For larger cylinder wall spacing (G/D $\geq$ 2), the cylinders are outside of the boundary layer formed on the plane wall and positive vorticies also appear in the wake region while boundary layer formed on the plane wall merges with the vorticies in the downstream region. The appearance of the isotherms behind the cylinders (right column) resemble to the isovorticity curves.

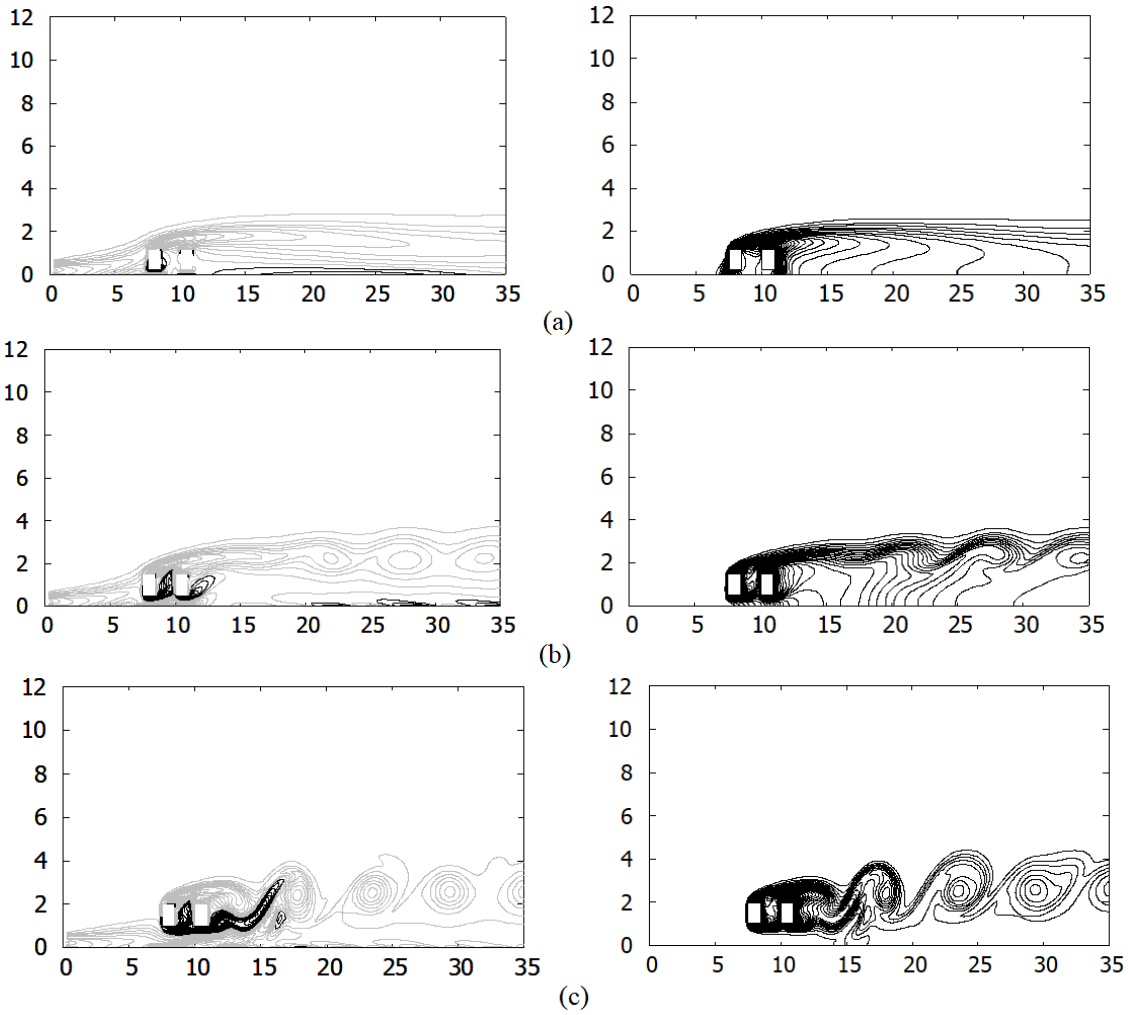

Figure 3. (cont.)

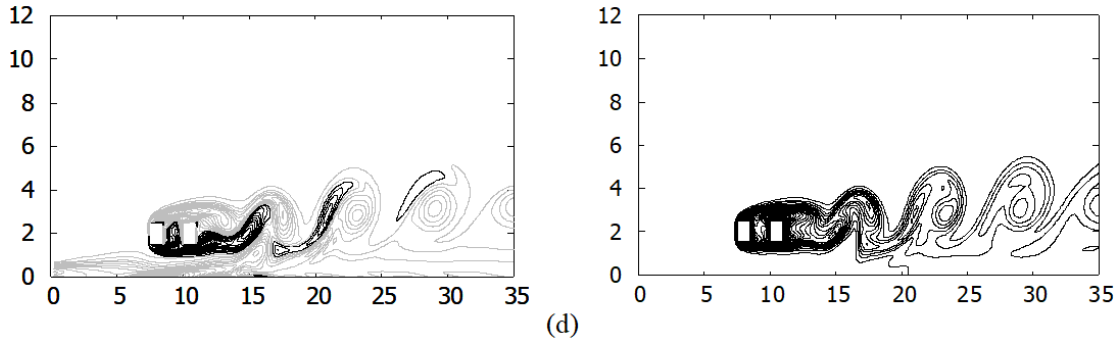

(d)

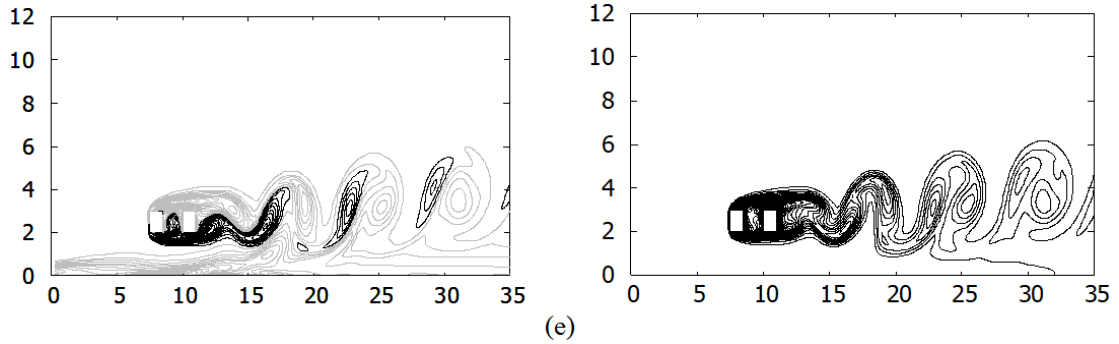

(e)

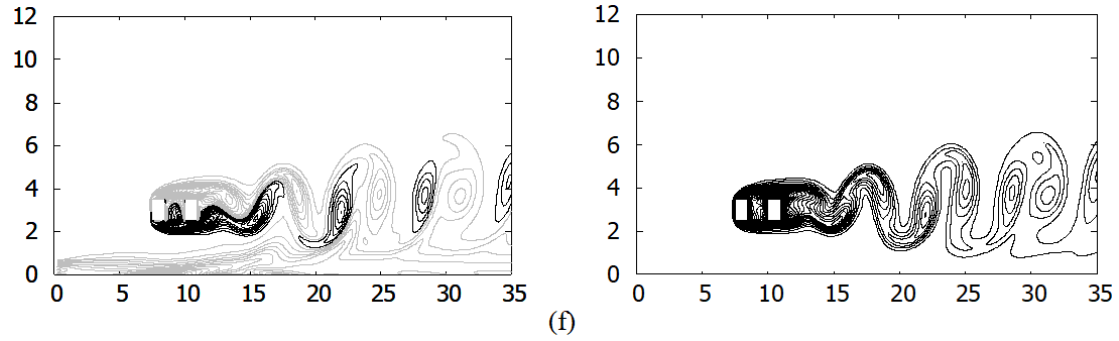

(f)

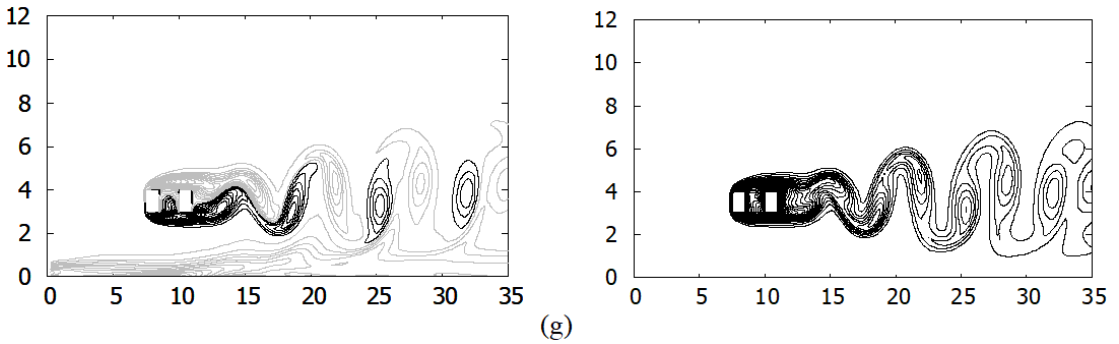

(g)

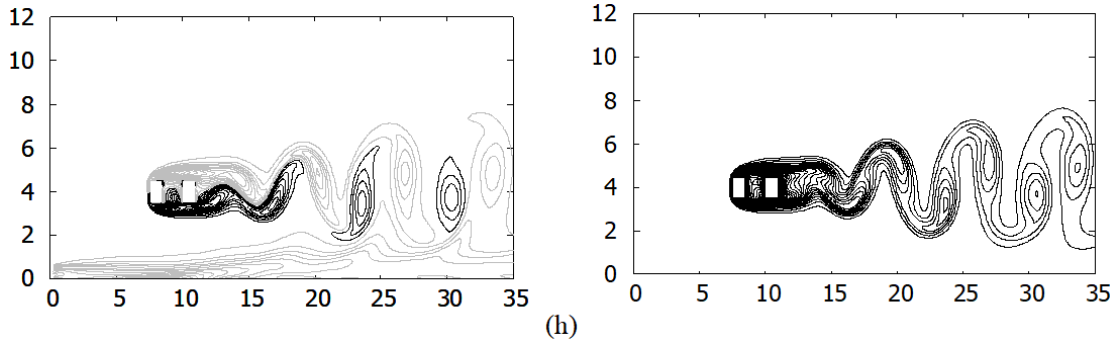

(h)

Figure 3. (cont.)

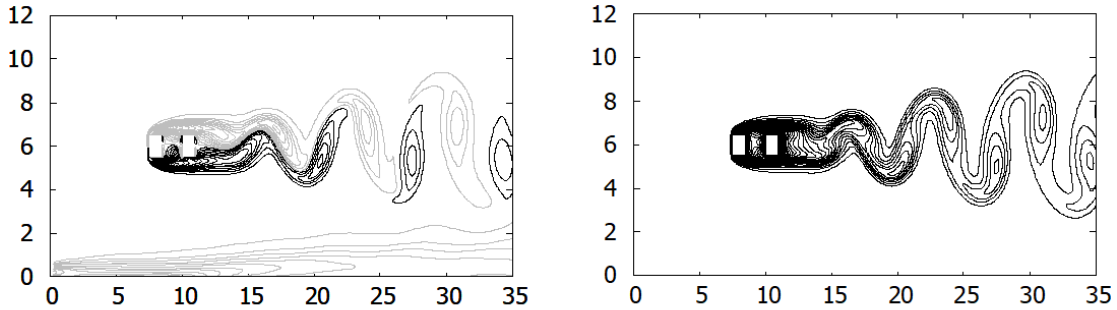

(ı)

Figure 3. Vorticity for tandem arrangement of two cylinders with the wall (L = 1.5 D): a) G/D = 0.7, b) G/D = 1, c) G/D = 1.5, d) G/D = 2, e) G/D = 2.5, f) G/D = 3, g) G/D = 3.5, h) G/D = 4, ı) G/D = 6.Gray and black lines present the negative and positive vorticities respectively. (Left and right columns present the isovorticities and the isotherms respectively. Axial and normal coordinates corresponds to x and y respectively.)

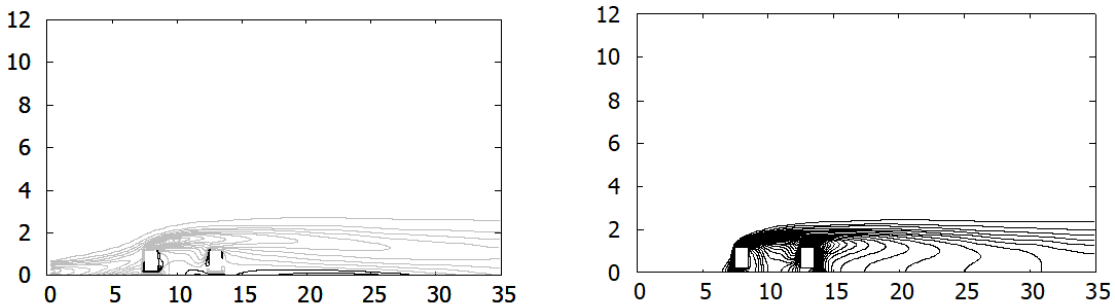

(a)

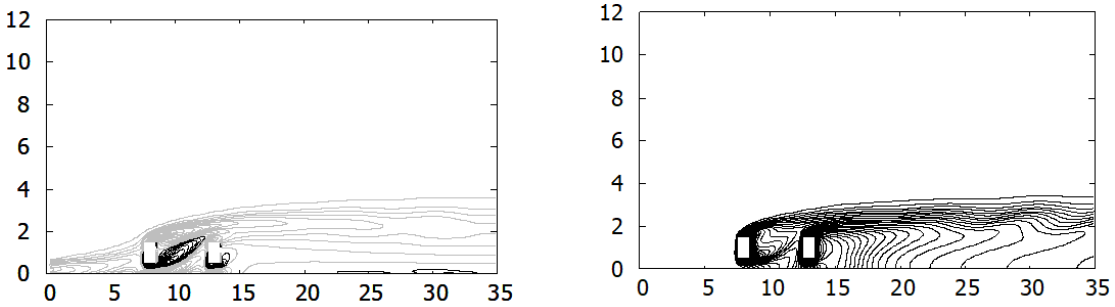

(b)

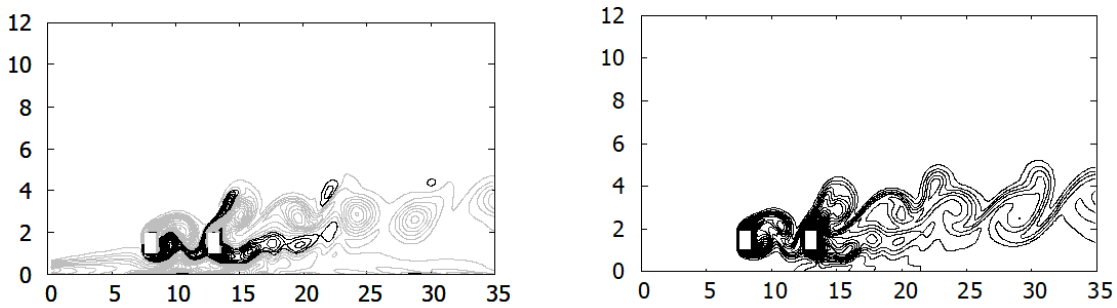

(c)

Figure 4. (cont.)

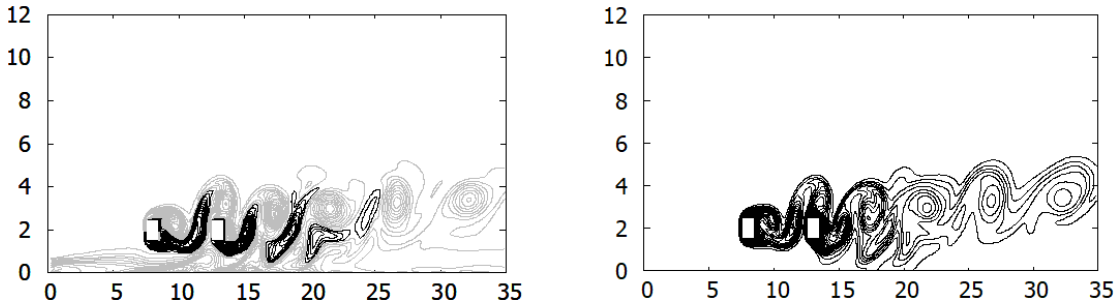

(d)

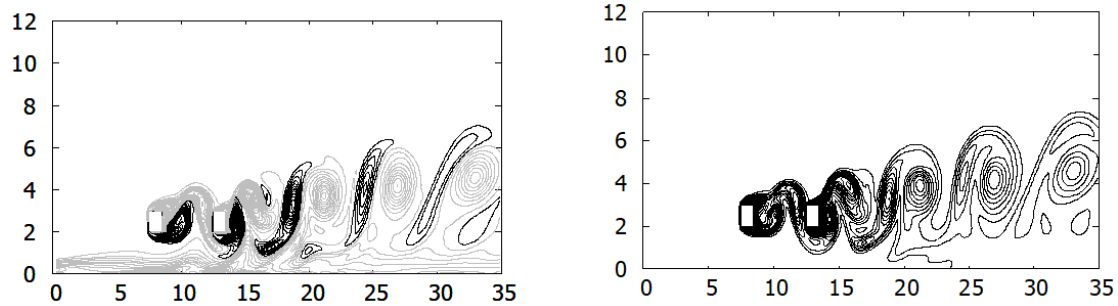

(e)

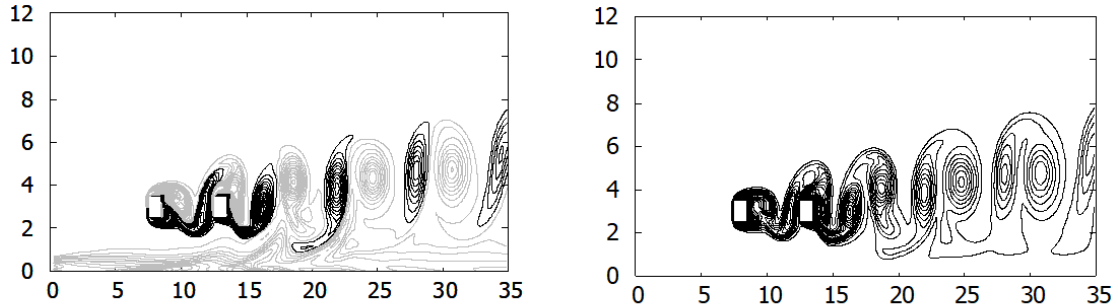

(f)

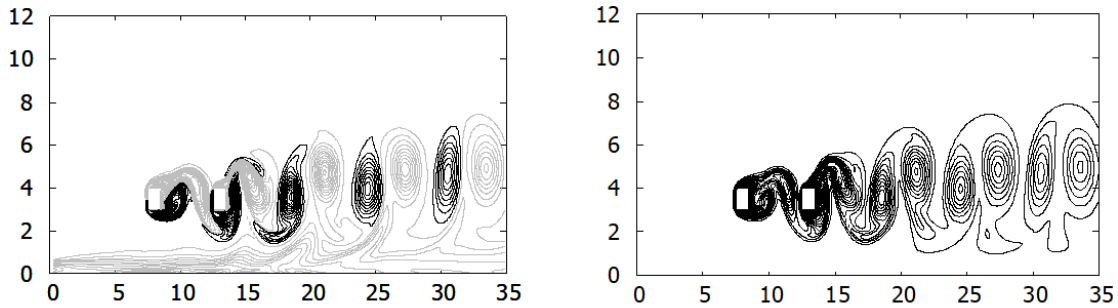

(g)

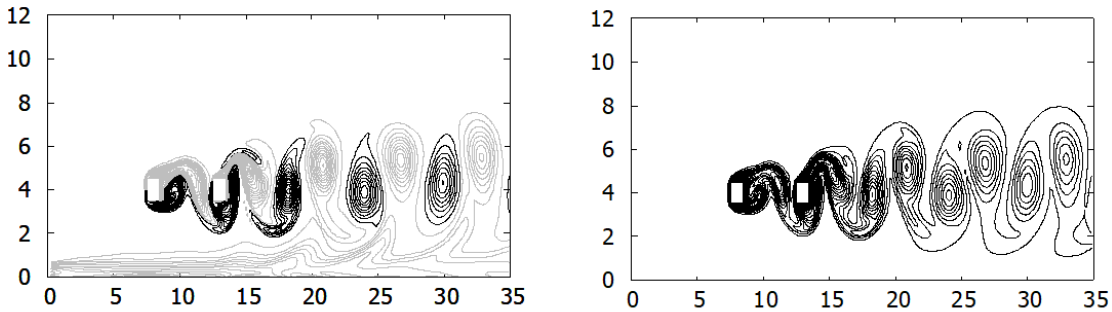

(h)

Figure 4. (cont.)

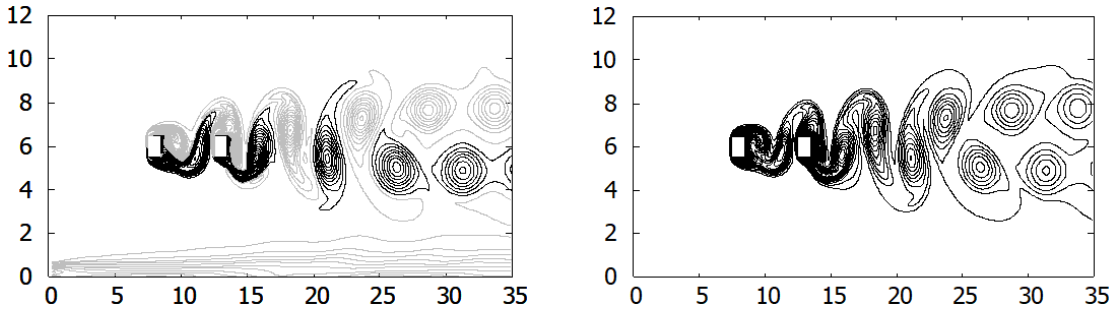

(ı)

Figure 4. Vorticity for tandem arrangement of two cylinders with the wall (L = 4D): a) G/D = 0.7, b) G/D = 1, c) G/D = 1.5, d) G/D = 2, e) G/D = 2.5, f) G/D = 3, g) G/D = 3.5, h) G/D = 4, ı) G/D = 6. Gray and black lines present the negative and positive vorticities respectively. (Left and right columns present the isovorticities and the isotherms respectively. Axial and normal coordinates corresponds to x and y respectively.)

In Figure 4, instantaneous vortex structure and isotherms were provided for larger spacing of the cylinders (L/D = 4). In small gaps (G/D = 0.7 and 1), the cylinders were within the oncoming boundary layer, and this leads to flow with smaller velocities around the cylinders, resulting suppression of vortex formation between the cylinders (Figures 4a, b).

For G/D = 1.5, although cylinders were partially inside of the oncoming boundary layer, the velocities around the cylinders were high enough to produce vortices in the gap of cylinders (Figure 4c) while positive vorticies formed from down edge of the cylinders disappear in the wake region where negative ones become dominant. For larger distances (G/D ≥ 2), the positive vorticies diffuse further downstream region. It is evident that the weaker wall effect yields stronger positive vortex in the downstream of cylinders (Figures 4e-i). While regular type Karman vortex street formed in the wake of cylinder at G/D = 2.5-4 (Figures 4e-h), a pair of row with a positive and negative vortex lines observed at G/D = 6 (Figure 4i). At this cylinder to cylinder spacing, the isotherms between the cylinders and in the wake region similar to the isovorticity contours (Figure 4 left column).

Unsteady Forces

In Figure 5, mean and root mean square values of C_L on the both cylinders were provided for the range of cylinder spacing L/D = 1.5, 2.5, 4 and cylinder wall gap ratio of G/D = 0.7-6. On the upstream cylinder, the mean lift coefficients reach their maximum values at G/D = 0.7 (Figure 5a), where the cylinders are inside the boundary layer formed on the plane wall (Yetik, 2013). Large differences between the velocities upper and lower side of the upstream cylinder lead to large deviations at G/D = 0.7. As G/D increases, the mean lift coefficient drops sharply. For G/D ≥ 2, the cylinders were outside of the plane wall boundary layer so that the differences between the velocities upper and lower side of the cylinders were small and the mean lift coefficients on the upstream cylinders takes small values. The lift coefficient reaches maximum values at G/D = 1 on the downstream cylinder. Large value of the mean lift coefficient observed on the downstream cylinder for L/D = 1.5 where boundary layer separated from upstream cylinder overshoot the downstream one (Figure 3). The root mean square values of the lift coefficients are more sensitive to cylinder-wall distances when cylinders are in boundary layer or partially in it (Figure 5b). For G/D < 2, C_{Lrms} values increase more rapidly with increasing G/D. For G/D ≥ 2, these values are affected by the distance between the cylinders rather than the plane wall. The shear layer separated from upstream cylinder provides more oscillatory velocities and pressures on the upper and lower side of the downstream cylinder, resulting in larger C_{Lrms} values on the downstream cylinder.

The C_{Dmean} and C_{Drms} values obtained at different wall to cylinder distances are depicted in Figure 6 for L/D = 1.5, 2.5 and 4. For upstream cylinders (Figure 6a), the variation of the C_{Dmean} value greatly depends on whether cylinder is inside or outside of the coming boundary layer. When the cylinder is within the boundary layer (G/D ≤ 1.5), C_{Dmean} value increases with increasing G/D, while slightly decreases for G/D > 1.5. The C_{Dmean} value on the upstream cylinder slightly changes with L/D indicating that the flow structure between the cylinders has weak upstream effect on drag force. C_{Dmean} values on the downstream are more sensitive to flow between the cylinders. For L/D ≥ 2.5, vortex forms between the cylinders and formed vortices strikes the front surface of downstream cylinder yielding larger C_{Dmean} mean values. The root mean square value of the drag force on the upstream cylinder is also slightly influenced by the flow between the cylinders while it take largest values at L/D = 2.5. C_{Drms} values on the downstream cylinder yields the largest values at L/D = 2.5 and 4 at which vortex street forms between the cylinders. When the cylinders are within the boundary layer, C_{Drms} value on the downstream cylinder increases rapidly as G/D increases (Figure 6b)

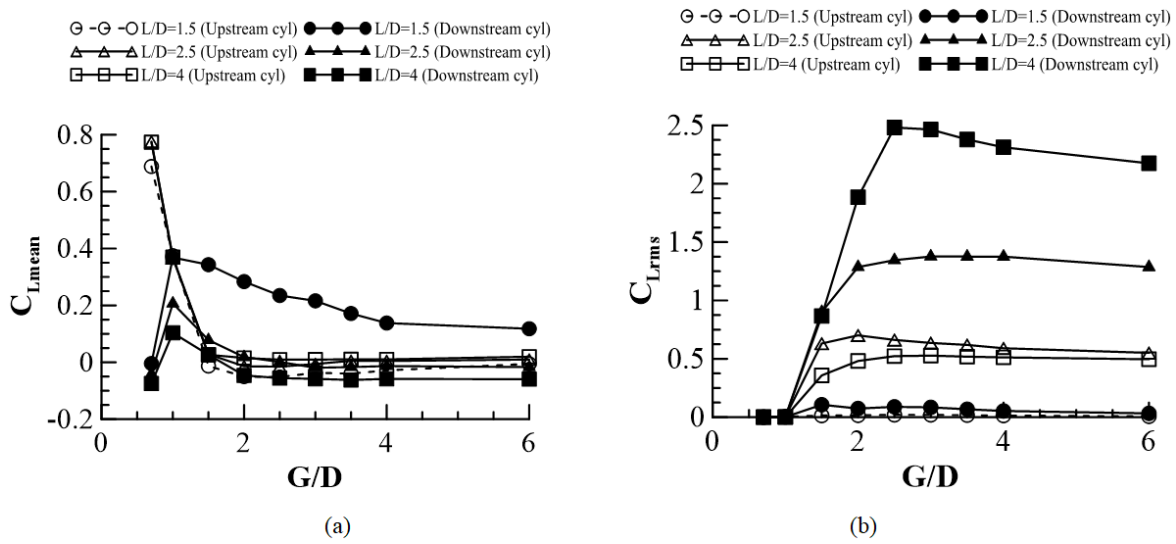

Figure 5. Variation of the mean lift coefficient (a), the root mean square value of lift coefficient (b) with the G/D values.

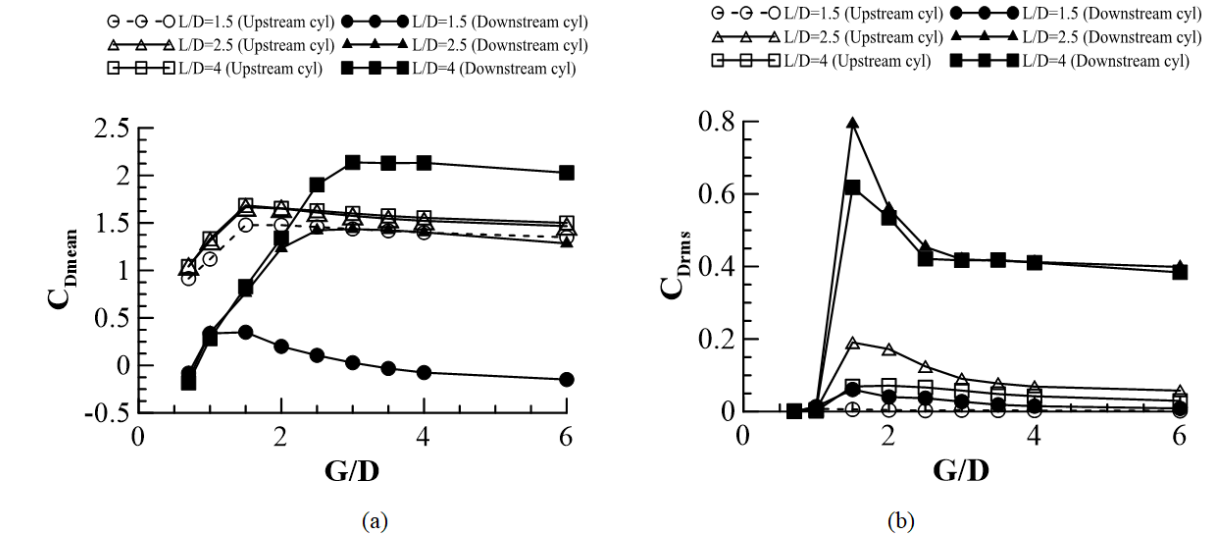

Figure 6. Variation of the mean drag coefficient (a), mean square value of drag coefficient (b) with the G/D values.

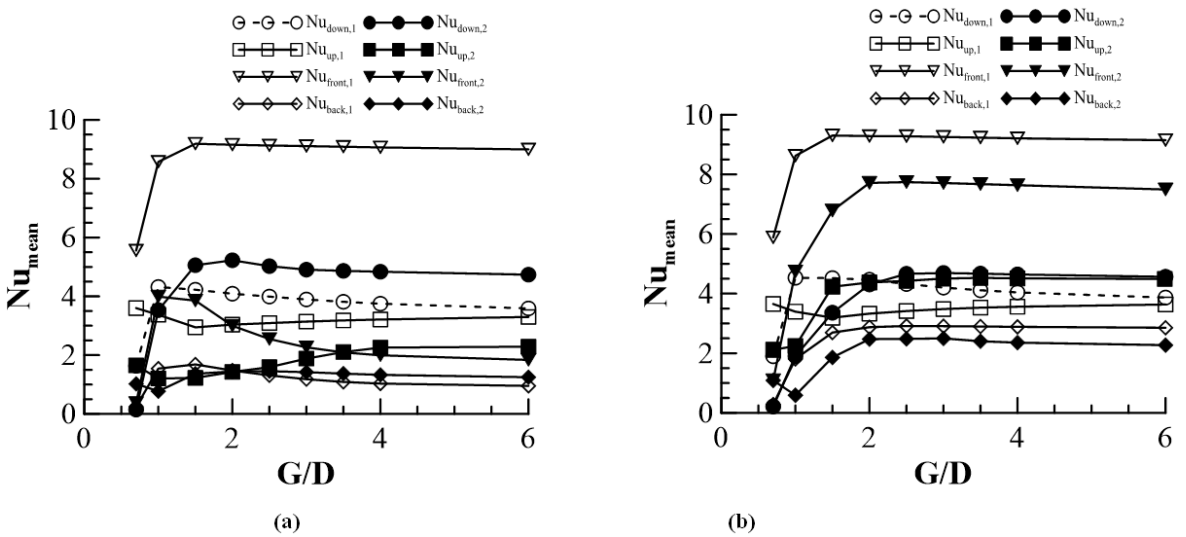

Figure 7. Variation of the Nusselt number for each of cylinder faces for L/D = 1.5 (a) and for L/D = 4 (b).

Variation of Mean Nusselt Number On The Cylinder Surfaces

Variation of the mean Nusselt number on the surfaces of up and downstream cylinders were provided in Figure 7 for L/D = 1.5 and 4. The heat transfer from cylinder surfaces sensitive to cylinder-plane wall distances. For G/D ≥ 2 the mean Nusselt numbers on the back, up and down surface of the upstream cylinders are approximately same at both L/D ratios, indicating that when the cylinders are outside of the oncoming boundary layer, the distance between the cylinders do not have distinct effect on the heat transfer from these surfaces whereas the heat transfer from front surface is higher for L/D = 4. For both L/D ratios, the Nusselt number on the down surface of upstream cylinder is larger than that on the up one due to jet like flow between plane wall and cylinders. As the cylinder plane wall distance increases, the mean Nusselt values on the up surface of the upstream cylinder approximate those of the down surface. For downstream cylinders, the heat transfer from surfaces is largely dependent on the flow between the cylinders at G/D ≥ 2. For L/D = 1.5, the Nusselt number on the front surface has relatively smaller values due to over shooting or reattachment flow between the cylinders (Figure 3), while it takes larger values for L/D = 4 where vortex forms between cylinders (Figure 4).

Local Nusselt Numbers On The Cylinder Surfaces

The convective heat transfer from cylinder surfaces also depends on the flow around the cylinders and between the cylinder-plane wall. Figures 8 and 9 present the variation of the mean Local Nusselt numbers on both cylinders with the plane wall distances for L/D = 1.5.

On the upstream cylinder, smaller values of Nusselt numbers were observed when the cylinders were inside the boundary layer formed on the plane wall G/D = 0.7 (Figure 8). On the down surface, it takes larger values at G/D = 1 due to jet like flow between cylinder and wall. At G/D = 2 and 4, the cylinders were outside the oncoming boundary layer, and the flow hits the front surface and deflects up and down, causing greater heat transfer near the corners of this surface.

For G/D = 0.7, the heat transfer from front and down surface of the downstream cylinder is approximately zero (Figure 9) due to very low flow velocities in the gap of downstream cylinder - plane wall. The Nusselt numbers take the maximum values on the front surface when the cylinders are still inside the oncoming boundary layer at G/D = 1. Further distance to plane wall leads to drop on the Nusselt number on this surface. For G/D = 1, 2 and 4; the greatest values of the Nusselt numbers were observed at the common edges of the front and bottom surface since the jet flow formed between the upstream cylinder and the plane wall directed to these surfaces (Figure 9). At the back and up surfaces Nusselt numbers are relatively small.

Figures 10 and 11 provide local Nusselt number variations on the cylinder surfaces for L/D = 4 where the vortex formed between the cylinders (Figure 4). For L/D = 1.5 and 4 cases, the comparison of Nusselt number variations on the upstream cylinder shows that the flow structure between the cylinders has negligible effect on the heat transfer from the front, bottom and top surfaces (Figures 8 and 10).

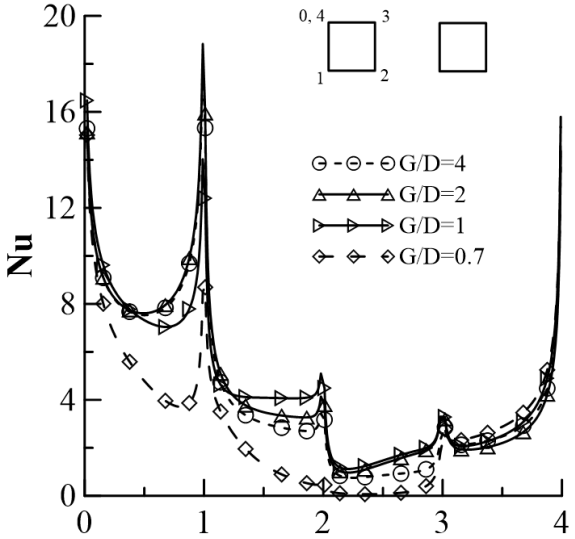

Figure 8. Local Nu values on the surfaces of upstream cylinder at L/D = 1.5, G/D = 0.7, 1, 2, and 4.

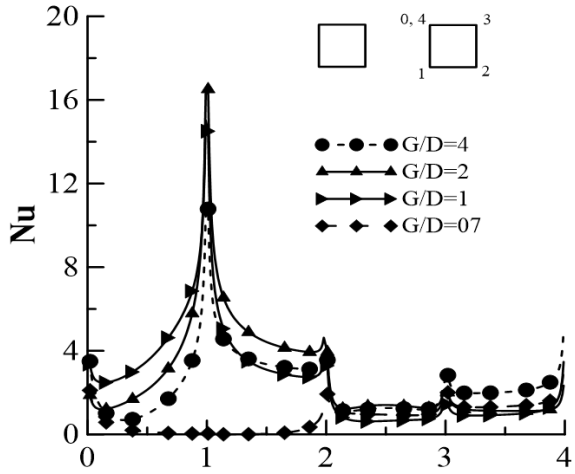

Figure 9. Local Nu values on the surfaces of downstream cylinder at L/D = 1.5, G/D = 0.7,1, 2, 4.

For G/D = 0.7, the Nusselt numbers variation on back surface are approximately same for both cases. For L/D = 4, while the cylinders are within the coming boundary layer, the Nu number increases as the G/D increases on the back surface of the upstream cylinder and becomes approximately twice that for L/D = 1.5 when the cylinder is just outside the boundary layer (G/D = 1) (Figure 10). The variation of Nusselt number on the downstream cylinder surfaces is given in Figure 11 for L/D = 4. While the cylinders are outside the oncoming boundary layer (G/D = 2, 4), the variation of the Nusselt number on the front surface of the upstream cylinder is somewhat unaffected by the cylinder plane wall distances, but on the other surfaces it slightly varies. When the cylinders

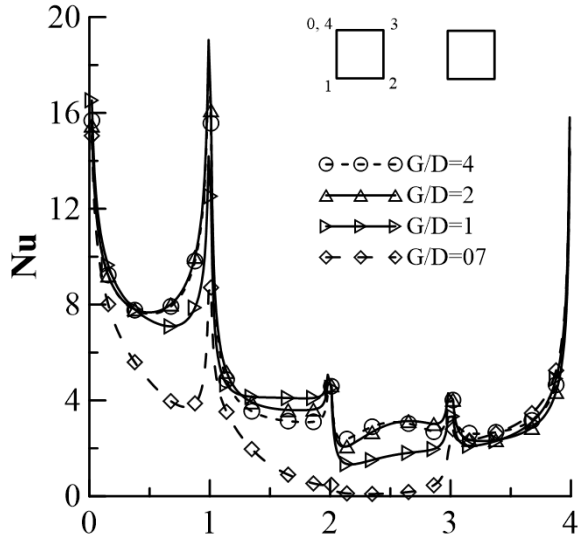

Figure 10. Local Nu values on the surfaces of upstream cylinder at L/D = 4, G/D = 0.7, 1, 2, and 4.

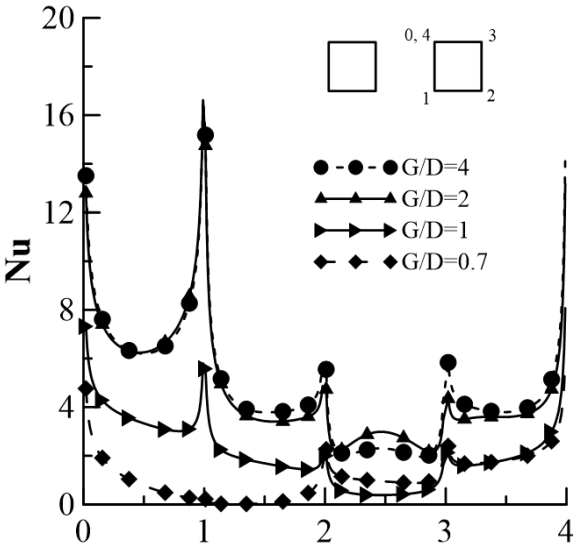

Figure 11. Local Nu values on the surfaces of downstream cylinder at L/D = 4, G/D = 0.7, 1, 2, and 4.

are in the boundary layer, the Nusselt numbers take lower values for the front and top surfaces at G/D = 0.7, for which flow velocities have relatively smaller values. On the downstream cylinders, Nusselt numbers is less sensitive to the distance between the cylinders (Figures 9 and 11) for G/D = 0.7, due to fact that both upstream and downstream cylinders are inside of the oncoming boundary layer. Other noticeable difference appears at the variation of Nusselt number on the front surfaces of downstream cylinders at G/D = 4 (Figures 9 and 11). At this G/D ratio, flow between the cylinders differs depending on the distance between the cylinders (Figure 3h and Figure 4h). For L/D = 4, shedding vortices from upstream cylinder pass through up and down side of the downstream cylinder alternately and leads nearly symmetrical Nu variation about the centerline although it is non symmetrical for L/D = 1.5. At the same time, vortex shedding between the cylinders also leads Nu values become larger on the surfaces of downstream cylinders for L/D = 4 than that for L/D = 1.5.

CONCLUSION

In this study, the flow around two heated tandem cylinders near a plane wall and the convective heat transfer from these cylinders were investigated numerically for Re = 150 and Pr = 0.71. The distance between the cylinders are selected as L/D = 1.5, 2.5 and 4 while the gap ratios between the cylinders varied as G/D = 0.7, 1, 1.5, 2, 2.5, 3, 3.5, 4 and 6. The vorticity and coincident temperature curves are obtained to understand and interpret flow and heat transfer. It is possible to separate the distance between the plane wall and cylinders to three regions as close proximity, moderate proximity and far proximity regions.

At close proximity region, the gap between the cylinder and wall is small (G/D ≤ 1), the cylinders inside of the coming boundary layer and around the cylinder, the flow velocities are relatively low. There are approximately no oscillations in the drag and lift coefficients of the upstream and downstream cylinders, and values of approximately zero C_{Lrms} and C_{Drms} occur. In the close proximity region, mean values of the lift coefficients on the upstream cylinder takes their largest values and decrease by the increasing G/D ratio, while these values are very low on the downstream one and increase by the increasing G/D (Figure 5a). In this region (G/D ≤ 1), the mean Nusselt numbers on the left and down surfaces also sharply increased with increasing G/D while it slightly varies on the up surfaces of both cylinders (Figure 7a). At moderate proximity region, cylinders are still inside of the approaching boundary layer. For both cylinders, the C_{Dmean} values increases while C_{Lmean} values continuous to drop until G/D = 1.5. At far proximity region, variations of flow and heat transfer characteristics on the both cylinders are less sensitive to the cylinder plane wall distances especially for G/D > 2.5.

REFERENCES

Armfield, S. W and Street, 2000, Fractional step methods for the Navier-Stokes equations on non-staggered grids, *ANZIAM journal*, Vol. 42, pp. C134-C156.

Bhattacharyya, S. and Maiti, D. K., 2004, Shear flow past a square cylinder near a wall, *International Journal of Engineering Science*, 42, 2119-2134.

Chatterjee, D. and Amiroudine, S., 2010, Two-dimensional mixed convection heat transfer from confined tandem square cylinders in cross-flow at low Reynolds numbers, *International Communications in Heat and Mass Transfer*, 37, 7-16.

Chatterjee, D., Biswas, G. and Amiroudine, S., 2009, Numerical investigation of forced convection heat transfer in unsteady flow past a row of square cylinders, *International Journal of Heat and Fluid Flow*, 30, 1114-1128.

Chatterjee, D., and Mondal, B., 2012, Forced convection heat transfer from tandem square cylinders for various spacing ratios, *Numerical Heat Transfer,Part A: Applications*, 61, 381-400.

Franke, R., Rodi, W. and Schönung B., 1990, Numerical calculation of laminar vortex shedding flow past cylinders, *Journal of Wind Engineering and Industrial Aerodynamics*, 35, 237-257.

Harichandan, A. B., and Roy, A., 2012, Numerical investigation of flow past single and tandem cylindrical bodies in the vicinity of a plane wall, *Journal of Fluids and Structures*, 33, 19-43.

Lei, C., Cheng, L., Armfield, S.W.K., Kavanagh, K., 2000. Vortex shedding suppression for flow over a circular cylinder near a plane boundary. *Ocean Engineering* Vol. 27, pp. 1109–1127.

Luo, S. C., Chew, Y. T. and Ng, T. T., 2003, Hysteresis phenomenon in the galloping oscillation of a square cylinder, *Journal of Fluids and Structures*, 18, 103-118.

Mahir, N., 2009, Three-dimensional flow around a square cylinder near a wall, *Ocean Engineering*, 36, 357-367.

Mahir, N. and Altaç, Z., 2008, Numerical investigation of convective heat transfer in unsteady flow past two cylinders in tandem arrangements, *International Journal of Heat and Fluid Flow*, 29, 1309-1318.

Malavasi, S. and Trabucchi, N., 2008, Numerical investigation of the flow around a rectangular cylinder near a solid wall, *BBAV. VI International Colloquium on: Bluff Bodies Aerodynamics & Applications* Milano, Italy, July, 20-24 2008.

Raiola, M., Ianiro, A. and Discetti, S., 2016, Wake of tandem cylinder near a wall, *Experimental Thermal and Fluid Science*, 8, 354-369.

Robichaux, J., Balachandar, S. and Vanka, S. P., 1999, Three-dimensional Floquet instability of the wake of square cylinder, *Physics of Fluids*, 11, 560–578.

Sahu, A. K., Chhabra, R. P. and Eswaran, V., 2009, Effects of Reynolds and Prandtl number on heat transfer from a square cylinder in the unsteady flow regime, *International Journal of Heat and Mass Transfer*, 52, 839-850.

Samani, M. and Bergstrom, D. J., 2015, Effect of a wall on the wake dynamics of an infinite square cylinder, *International journal of Heat and Fluid Flow*, 55, 158-166.

Schlichting, H., *Boundary layer theory*, 1979, Seventy ed. Mc Graw-Hill Book Company, NewYork.

Sharma, A. and Eswaran, V., 2004, Heat and fluid flow across a square cylinder in the two-dimensional laminar flow regime, *Numerical Heat Transfer, Part A: Applications*, 45, 247–269.

Shimizu, Y. and Tanida, Y., 1978, Fluid forces acting on cylinders of rectangular cross section, *Transc JSME B* 44, 2699–2706.

Sohankar, A., Davidson, L. and Norberg, C., 1995, Numerical simulation of unsteady flow around a square two-dimensional cylinder, *Twelfth Australasian Fluid Mechanics Conference, The University of Sydney*, Australia, 517-520.

Sohankar, A. and Etminan, A., 2009, Forced-convection heat transfer from tandem square cylinders in cross flow at low Reynolds numbers, *International Journal For Numerical Methods in Fluids*, 60, 733-751.

Sohankar, A., Norberg, C. and Davidson, L., 1997, Numerical simulation of unsteady low-Reynolds number flow around rectangular cylinders at incidence, *Journal of Wind Engineering and Industrial Aerodynamics*, 69, 189-201.

Sohankar, A., Norberg, C. and Davidson, L., 1998, Low-Reynolds-number flow around a square cylinder at incidence: study of blockage, onset of vortex shedding and outlet boundary condition, *International Journal for Numerical Methods in Fluids*, 26, 39–56.

Tang, G., Chen, C., Zhao, M. and Lu, L., 2015, Numerical simulation of flow past twin near-wall circular cylinders in tandem arrangement at low Reynolds number, *Water Science and Engineering*, 8, 315-325.

Wang, X. K., Hao, Z., Zhang, J. X. and Tan, S. K., 2014, Flow around two tandem square cylinders near a plane wall, *Experiments in Fluids*, pp. 55:1818.

Wang, X. K. and Tan, S. K., 2008, Near-wake flow characteristics of a circular cylinder close to wall, *Journal of Fluids and Structures*, 24, 605-627.

Yetik, O., 2013, Flow and heat transfer from two square cylinders, MSc Dissertation, Eskisehir Osmangazi University, Eskisehir, Turkey.